A Continuum Model for Condensation of DNA in Solution

YONGZHAO WANG
School of Mechanical Engineering
Tianjin Key Laboratory of
Nonlinear Dynamics and Chaos Control
Tianjin University
Weijin Road, Nankai District, Tianjin
CHINA
wangyongzhao1987@126.com

QICHANG ZHANG
School of Mechanical Engineering
Tianjin Key Laboratory of
Nonlinear Dynamics and Chaos Control
Tianjin University
Weijin Road, Nankai District, Tianjin
CHINA
Corresponding author: qzhang@tju.edu.cn

WEI WANG
School of Mechanical Engineering
Tianjin Key Laboratory of
Nonlinear Dynamics and Chaos Control
Tianjin University
Weijin Road, Nankai District, Tianjin
CHINA
wangweifrancis@163.com

DONGWEI HUANG
School of Science
Tianjin Polytechnic University
Binshui West Road, Xiqing District, Tianjin
CHINA
huangdongwei@tjpu.edu.cn

Abstract: As a coarse-gained model, an anisotropic super-thin elastic rod subjected to interfacial interactions is used to investigate the condensation of DNA segment. The interfacial pressure distributes on the surface of rod, and is determined in terms of the Young-Laplace equation. The influences of the interfacial factor, initial curvature, anisotropic bend ability and salt solution concentration on the formation of DNA segment are discussed, and DNA loop under different solution environment is studied. The simulated results show that DNA segment will undergo a series of alteration with the change of the solution environment, initial restriction, the shape of DNA rod cross-section and ionic strength. The total size of DNA segments under the interfacial energy and elastic strain reduce many times from the original shape, which is used to explain why several millimeter lengths of DNA can fit inside a cell of diameter 1 μm. The DNA loop exerts diverse forces upon the protein clamp at the end under different solution environment.

Key–Words: DNA configuration, Interfacial traction, Solution environment, Anisotropic modulus of DNA bending, DNA loop

1 Introduction

DNA is the primary genetic material of most organisms, which is a double helix. The study of DNA has attracted much attention in the last decades [1, 2, 3, 4, 5, 6, 7]. The mechanical deformation of DNA is important in many biological processes, such as genome packaging, DNA replication, and transcription. As misfolding of DNA has become the major cause of many illnesses, such as paroxysmal nocturnal hemoglobinuria (PNH) disease [1], and understanding the basic mechanisms of DNA folding could lead to new ways for preventing such diseases. The elastic rods provide idealized models to characterize both macroscopically and macrocosmically, such as flexible cables, antennas, shafts, pipes, proteins, DNA double helix and so on. The available approach to research these flexible structures need to assume that they are made of elasticity materials obeying the appropriate laws of elasticity. Mechanics for a super-thin rod with the biological background of DNA supercoiling macromolecules is an interdisciplinary frontier area of classical mechanics and molecular biology. Elastic theories have been widely used in studying the shape and deformation of its structures. Several important investigations have been done on the elastic properties of DNA chains, for example, refs [4, 5, 6, 7]. These results can provide insights into the mechanism of DNA.

With the advent of new modern techniques, such as force-measuring lasertwiizers [8], real-time fluorescence microscopy [25], and magnetic optical microscopy [10], researchers are presented with more opportunities to probe into the microstructure of in-

dividual great molecules than ever before. The ever growing volume of experimental data and experimental phenomenon provides us with the probabilities to improve the existing theoretical models. Kirchhoff's theory of elastic rod can be easily applied to many systems with great success, leading to a simple and elegant way for developing some insight into possible behaviors of rods. This approach is used to research DNA configuration and successful explain many phenomena, which are observed in experiment [11, 12, 13, 14, 15].

Despite experimental information has offered the valuable and well understood dates on some aspects of the relation-ship between solution environment and DNA segment, many puzzling date still remain, and some data is lacking. The terrific advances of computer power and software efficiency, long-time phenomena such as DNA folding or phase transitions remain outside the limits of such approaches. Analytical models based on classical elasticity theory do not suffer from space or time limitations.

Sequence dependence and anisotropy of bending persistence length has been widely noticed in the base-pair steps approaches, in which relative rotation and displacement of every two segments are defined trough six parameters slide, shift, rise, tilt, roll and twist [16]. These sequences dependent parameters for individual base-pair steps had been determined from their standard deviation in crystal complexes [17]. Anisotropic modulus of DNA bending are introduced in our model, which is more reasonable for description of DNA cross-section than the isotropic.

It is well known that DNA is always in intracellular solution. The conformational change between B-DNA and Z-DNA was first discovered in 1972 by Pohl and Jovin [10]. This transition could be involved in the control of the structural state of the chromosomes which depends on several experimental parameters, such as temperature and salt concentration [18]. Gil Montoro and Abascal [19] computed the free energies of the transitions between B- and Z-DNA through a thermodynamic route method which is called setup and charge (SUCH) method. The change of solution leads to the change of the DNA-solution interaction. The interaction of the DNA chain with the intracellular solution is a very important determinant of the DNA configuration. Thus, it is necessary to involve this interaction into DNA theoretical models.

The layout of this paper is as follows. Firstly, in the next section, a model, including DNA-solution interaction is introduced, and equilibrium configuration equations of DNA are proposed. Section 3 numerically simulates DNA reconfiguration. Finally, some conclusions are drawn.

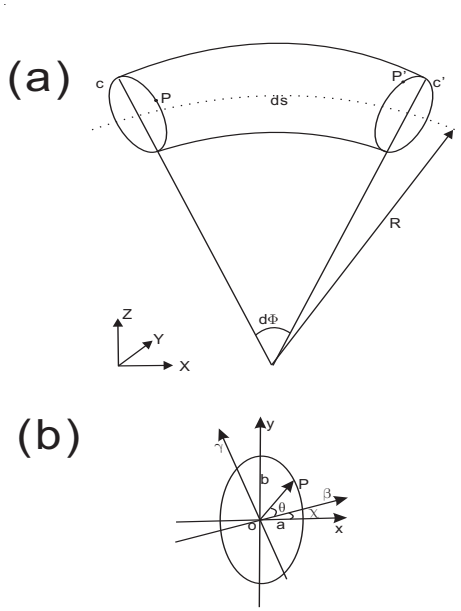

Fig. 1: (a) A fragment of DNA elastic rod with the elliptical cross-section, the length of central line ds,$C$and C' are the cross sections on the two ends. (b) The left cross section of the rod. When the cross section moves along the central line from the left end to the right end, P changes toP'.

2 The Elastic Rod Model For DNA

As a coarse-grained description, a DNA can be approximately regarded as a thin flexible and inextensible rod or string [12, 13, 14]. The classical theory of elasticity describes the geometry of an elastic rod in terms of its centerline $\boldsymbol{R} = (x(s), y(s), z(s))$, a three-dimensional curve parameterize by its arclength s. And a frame of three unit vectors $\boldsymbol{\alpha}$, $\boldsymbol{\beta}$, $\boldsymbol{\gamma}$ associated with each cross section of the rod, where $\boldsymbol{\alpha} = \dot{\boldsymbol{R}}$ be the tangent vector ($\dot{\boldsymbol{R}}$ denotes the derivative of $\boldsymbol{R}$ with respect to s which is the arclength of the central line of the rod), $\boldsymbol{\beta} = \dot{\boldsymbol{\alpha}}$ be the main normal vector and $\boldsymbol{\gamma} = \boldsymbol{\alpha} \times \boldsymbol{\beta}$ be the binormal vector, between those unit vectors, these are the Frenet formulaes: $d\boldsymbol{\alpha}/ds = \kappa\boldsymbol{\beta}$, $d\boldsymbol{\beta}/ds = -\kappa\boldsymbol{\alpha} + \tau\boldsymbol{\gamma}$ and $d\boldsymbol{\gamma}/ds = -\tau\boldsymbol{\beta}$, where κ and τ are the curvature and torsion of the central line $\boldsymbol{R}$, respectively [20]. In local orthonormal basis O-xyz, the $x-$ and $y-$ axes are the two principal inertial axes of the cross-section through the point O. The angle between the principal normal $\boldsymbol{\beta}$ and the x-axis (or the binormal $\boldsymbol{\gamma}$ and y-axis) is called the twisting angle, denoted by χ. The cross section is elliptical due to the anisotropic modulus of DNA bending, and the semi axis lengths of ellipse are a and b.

As shown in Fig. 1, point P is fixed on the cross section ring (on the left end of the rod) and the angle between $\overrightarrow{OP}$ and $\boldsymbol{\beta}$ is θ. When the cross section ring

moves along the central line from the left end to the right end, P changes to P'. For convenience we will study a simplified 2D model which is referred in ref [11]. It follows that $\tau = 0$ and $\chi = 0$. In this process, the angular displacement of point P in the local coordinates (x, y, z) is $d\theta$. The shape of the rod surface can be obtained by this way: the central point of a ring with the elliptical cross-section moves along a line $\boldsymbol{R}$ and keeps the ring upright to the tangent of $\boldsymbol{R}$. It means the ring is in the normal plane of the central line $\boldsymbol{R}$. Let $\boldsymbol{Y}$ be the shape of the rod surface, there is

$$\boldsymbol{Y} = \boldsymbol{R} + \boldsymbol{r} = \boldsymbol{R} + a\cos\theta\boldsymbol{\beta} + b\sin\theta\boldsymbol{\gamma}, \quad (1)$$

where the parameter $0 \leq \theta < 2\pi$, and $b \geq a > 0$.

Making use of the Frenet formulae, we obtain the first fundamental quantity of surface

$$\begin{aligned} E &= \boldsymbol{Y}_s \cdot \boldsymbol{Y}_s = (1 - a\kappa\cos\theta)^2, \\ F &= \boldsymbol{Y}_s \cdot \boldsymbol{Y}_\theta = 0, \\ G &= \boldsymbol{Y}_\nu \cdot \boldsymbol{Y}_\theta = a^2\sin^2\theta + b^2\cos^2\theta, \end{aligned} \quad (2)$$

where $\boldsymbol{Y}_s = \frac{\partial \boldsymbol{Y}}{\partial s}$.

The second fundamental quantity of surface

$$\begin{aligned} L &= \boldsymbol{Y}_{s,s} \cdot \boldsymbol{n} = -\frac{b\kappa\cos\theta(1-a\kappa\cos\theta)}{\sqrt{a^2\sin^2\theta + b^2\cos^2\theta}}, \\ M &= \boldsymbol{Y}_{s,\theta} \cdot \boldsymbol{n} = 0, \\ N &= \boldsymbol{Y}_{\theta,\theta} \cdot \boldsymbol{n} = \frac{ab}{\sqrt{a^2\sin^2\theta + b^2\cos^2\theta}}, \end{aligned} \quad (3)$$

where $\boldsymbol{n}$ is the main normal vector of the rod surface

$$\begin{aligned} \boldsymbol{n} &= \frac{\boldsymbol{Y}_s \times \boldsymbol{Y}_\theta}{|\boldsymbol{Y}_s \times \boldsymbol{Y}_\theta|} \\ &= \left\{0, \frac{-b\cos\theta}{\sqrt{H}}, \frac{-a\sin\theta}{\sqrt{H}}\right\}, \end{aligned} \quad (4)$$

where $H = a^2\sin^2\theta + b^2\cos^2\theta$.

Consequently we can easily get the mean curvature at the point P

$$\begin{aligned} \Lambda &= \frac{LG - 2MF + NE}{2(EG - F^2)} \\ &= \frac{b}{2\sqrt{H}}\left[\frac{-\kappa\cos\theta}{1 - a\kappa\cos\theta} + \frac{a}{H}\right]. \end{aligned} \quad (5)$$

In this paper, we characterize the interactions of DNA with solution by interfacial traction between a rod and the solution surrounding the rod, which is consistent with ref [11]. Following the Young-Laplace formula [21], the interfacial traction at point P reads

$$\begin{aligned} p &= \sigma(\kappa_1 + \kappa_2) = 2\sigma\Lambda \\ &= \sigma\frac{b}{\sqrt{H}}\left[\frac{-\kappa\cos\theta}{1 - a\kappa\cos\theta} + \frac{a}{H},\right] \end{aligned} \quad (6)$$

where p denotes the normal traction on the interfacial surface between the rod and the solution. κ_1, κ_2 are two principal curvatures of the surface at point P, and σ is the interfacial energy factor, which is a positive constant and represents a composite effect of hydrophilic and hydrophobic patches along the DNA surface, and relates to the solution environment.

In coordinates $P-xyz$, Eq. 6 can be decomposed into

$$\begin{aligned} p_1 &= -\sigma\frac{b}{\sqrt{H}}\left[\frac{-\kappa\cos\theta}{1-a\kappa\cos\theta} + \frac{a}{H}\right]\cos\theta, \\ p_2 &= -\sigma\frac{b}{\sqrt{H}}\left[\frac{-\kappa\cos\theta}{1-a\kappa\cos\theta} + \frac{a}{H}\right]\sin\theta, \\ p_3 &= 0. \end{aligned} \quad (7)$$

Integrate the above equations along the perimeter of the cross-section of the rod, through the software Mathematica 7.0, the traction on the central axis curve $\boldsymbol{R}(s,t)$ can be obtained

$$\begin{aligned} f_1 &= \int_0^{2\pi} -\sigma b\left[\frac{-\kappa\cos\theta}{1 - a\kappa\cos\theta} + \frac{a}{H}\right]\cos\theta d\theta \\ &= -\frac{b}{a}\frac{2\pi\sigma}{a\kappa}(1 - \frac{1}{\sqrt{1 - a^2\kappa^2}}), \\ f_2 &= \int_0^{2\pi} -\sigma b\left[\frac{-\kappa\cos\theta}{1 - a\kappa\cos\theta} + \frac{a}{H}\right]\sin\theta d\theta \\ &= 0 \\ f_3 &= 0 \end{aligned} \quad (8)$$

It is worth noting that the calculation of the interfacial traction is not correct in ref [11], $f_1 = \frac{2\pi\sigma}{r\kappa}(1 - \frac{1}{\sqrt{1-r^2\kappa^2}})$ when $a = b = r$. The miscalculation of the integration of Eq. (10) in ref [11] is the cause of the error. when the curvature $\kappa = 0$,

$$f_1(0) = \lim_{\kappa\to 0} -\frac{b}{a}\frac{2\pi\sigma}{a\kappa}(1 - \frac{1}{\sqrt{1 - a^2\kappa^2}}) = 0. \quad (9)$$

This is to say for a straight rod, the interfacial traction is zero, which is canceled out around the rod. However, zero is the singularity of $f_1 = \frac{2\pi\sigma}{r\kappa}$. The curvature cannot be zero, which is inconsistent with reality. In the following, the equilibrium configuration equations of the simplified model which follows that $\tau = 0$ and $\chi = 0$ can be get

$$\begin{aligned} &\frac{dF_1}{ds} + (\kappa_0 + \kappa)F_3 \\ &\quad -\frac{b}{a}\frac{2\pi\sigma}{a\kappa}(1 - \frac{1}{\sqrt{1-a^2\kappa^2}}) = 0, \\ &\frac{dF_3}{ds} - (\kappa_0 + \kappa)F_1 = 0, \\ &B\frac{d\kappa}{ds} + F_1 = 0, \\ &\frac{dx}{ds} = \cos\theta, \\ &\frac{dy}{ds} = \sin\theta, \\ &\frac{d\theta}{ds} = \kappa + \kappa_0, \end{aligned} \quad (10)$$

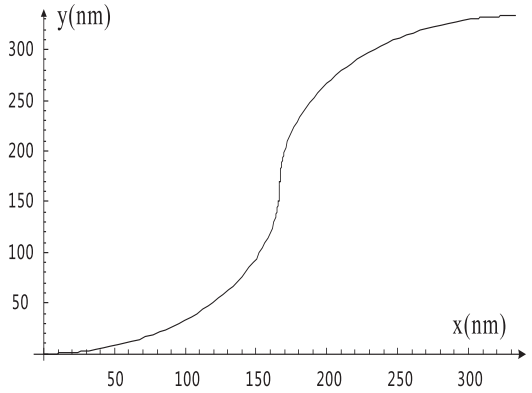

Fig. 2: Original configuration of a DNA segment.

where F_i $(i = 1, 3)$are the stress resultant acting at the center of cross section, κ_0 denotes the curvature of the original configuration of the rod. x, y are the horizontal and vertical coordinates of the central axis curve $\boldsymbol{R}$ in the plane, respectively. The bending stiffness $B = \pi E a^3 b/4$, and E is Young's modulus.

3 Numerical results

In this section, firstly, we use the values of ref [11] to numerically solve the above equilibrium configuration equations. The aim is to show the configuration under the correct interfacial traction. In ref [11], the initial condition is $F_1(0) = F_3(0) = 0$, $\kappa(0) = 0$, $x(0) = y(0) = 0$ and $\theta(0) = 0$.

3.1 The reconfiguration under correct traction

In this section, One can choose $a = b = 1nm$, the original configuration of a DNA segment consists of two inextensible circular one-quarter arcs, as shown in Fig. 2. The initial curvatures of both arcs are all 0.006 nm^{-1}, which is consistent with ref [11].

Consider the interfacial energy factor $\sigma = 5.0 \times 10^{-4} nN/nm$, and Young's modulus $E = 0.16 nN/nm^2$. Using the classical Runge-Kutta algorithm [22], we calculate the configuration corresponding to the original configuration in Fig. 2. From the result which is shown in Fig. 3, ones can see that the DNA segment does not coil into a "toroid" as shown in Fig 3(b) spontaneously. Clearly, the reconfiguration of DNA is different greatly with respect to Fig. 3(b). This shows that the interfacial traction has a significant influence on the conformation of DNA and the correct traction is important for the DNA configuration research. However, the shape of the DNA segment changes and the area occupied by the DNA segment decrease comparing with the original configuration. The reconfiguration of DNA segments differ with the one in ref [11] when $\sigma = 5.0 \times 10^{-6} nN/nm$, $E = 1.6 nN/nm^2$ and $\sigma = 5.0 \times 10^{-8} nN/nm$, $E = 16 nN/nm^2$, respectively.

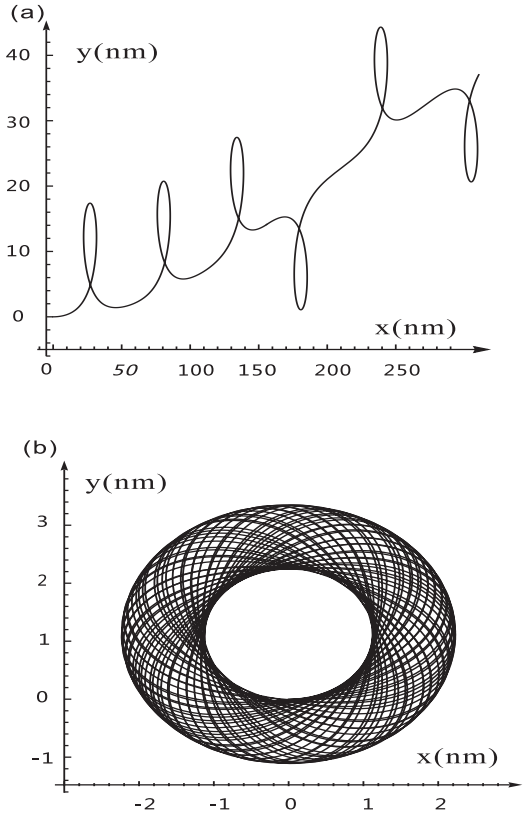

Fig. 3: (a)DNA configuration under revised traction. (b)DNA configuration under incorrect traction in ref [11] with $\sigma = 5.0 \times 10^{-6}$ nN/nm,$E = 1.6 nN/nm^2$.

Now, we take the value of the interfacial energy factor $\sigma = 4.5 \times 10^{-2}$ nN/nm, and Young's modulus $E = 1.6$ nN/nm^2, $a = 1$ nm, $b = 3/2$ nm, the original configuration is a semi-circular arcs with initial curvature 0.001 nm^{-1}. The result of DNA reconfiguration under interfacial energy factor $\sigma = 4.9 \times 10^{-2}$ nN/nm is shown in Fig. 4, the toroidal DNA are observed which was found by many investigators in experiments [23, 24, 25, 26] and its outer diameter is about 36.85 nm. This initial value problem of the equilibrium configuration equations is essentially one boundary value problem with the beginning endpoint fixed and another endpoint free. Next we study the effect of interfacial energy on the DNA reconfiguration. Fig.5 and 6 take the interfacial energy factor $\sigma = 4.6 \times 10^{-2}$ nN/nm and $\sigma = 4.2 \times 10^{-2}$ nN/nm, respectively. Fig. 4-6 reveal that DNA segments undergo different reconfiguration with different σ. How-

ever, the reconfigurations of DNA segments keep the ring in Fig. 5 and 6, and the outer diameter are about 50.77 nm and 75.44 nm, respectively.

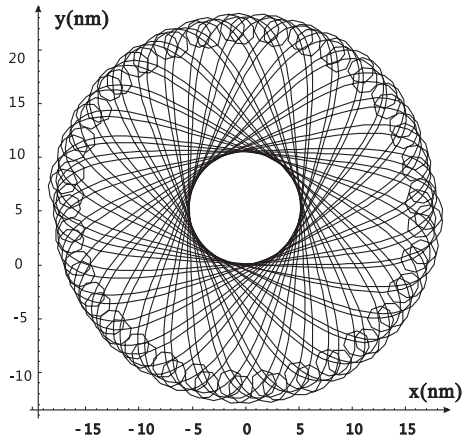

Fig. 4: DNA configuration with interfacial energy factor $\sigma = 4.9 \times 10^{-2}\ nN/nm$.

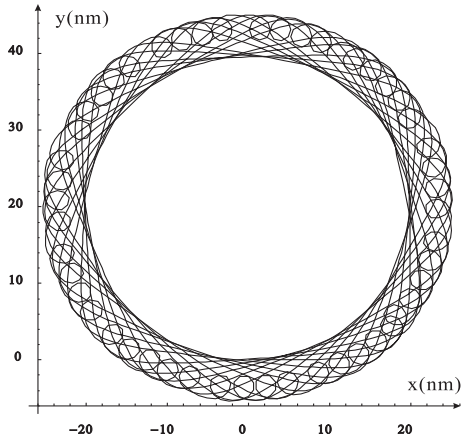

Fig. 5: DNA configuration with interfacial energy factor $\sigma = 4.6 \times 10^{-2}\ nN/nm$.

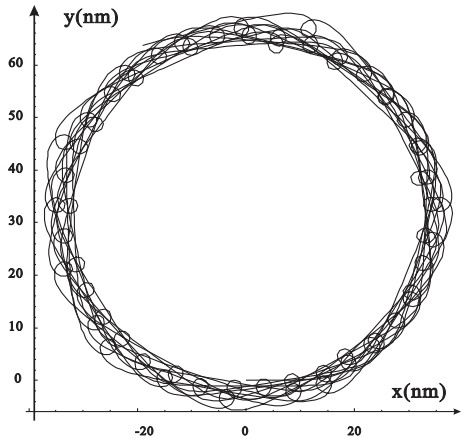

Fig. 6: DNA configuration with interfacial energy factor $\sigma = 4.2 \times 10^{-2}\ nN/nm$.

These show that interfacial energy is a significant factor for DNA configuration which is on behalf of different solution environments qualitatively. As is known that the interfacial tension between solution and DNA segment is difficult to measure [27], but $\kappa(0)$, Young's modulus E, the semi axis lengths of cross-section and the outer diameter of toroid are measured easily. If $\kappa(0)$ and E are known, we can estimate the interfacial tension according to the outer diameter of DNA toroid. This will provide a method to estimate the interfacial tension.

It is worth noting that the rod, which of one end of the rod is fixed and another free end, is controlled by the interfacial traction. In the following, we will discuss the effect of initial curvature on DNA configuration. we take the interfacial energy factor $\sigma = 4.0 \times 10^{-2}\ nN/nm$ and change the initial curvature $\kappa(0)$ in this section. When the initial curvature κ= 0, DNA configuration is shown in Fig. 7, which illustrates that the toroidal DNA is destroyed. However, when the initial curvature κ= 0.005 nm^{-1} and κ= 0.05 nm^{-1}, the reconfigurations of "toroid" are appeared in Fig. 8 and 9, and the outer diameter are about 53.68 nm and 28.31 nm, respectively. From Fig. 7-9, the configuration of DNA segment changes a lot, which means that the initial curvature is also a significant factor for DNA configuration and on behalf of the initial restriction.

3.2 Effects of anisotropic bendability

Until recently, the experimental data on DNA bending have been interpreted in terms of a single effective bending modulus [29], and many theoretical studies used the approximation of isotropically bendable DNA [12, 13]. However, the atomic structure of DNA helix exhibits two sugar-phosphate backbone strands separated by two grooves. Clearly, bending towards the grooves should cost less energy than bending over the backbone [28]. It is reasonable to assume that the cross-section is elliptic. In the following, we will discuss the effect elliptical cross-section on the reconfiguration of DNA segment.

Take the interfacial energy factor $\sigma = 4.0 \times 10^{-2}$ nN/nm and different semi axis lengths of ellipse. When a=1 nm and b=1.5 nm, DNA segment has appeared the shape of '8' as shown in Fig. 10. When a=1 nm, b=3 nm and a=1 nm, b=9 nm, the DNA segments appear the toroidal shape with the outer diameter of 90.21 nm and 80.44 nm, which are shown in Fig. 11 and 12, respectively. From Fig. 10-12, the shape of DNA segments undergoes essential different reconfiguration under the interfacial energy. Thus, it is very important for studying the reconfiguration of DNA segment to measure the cross-sectional shape.

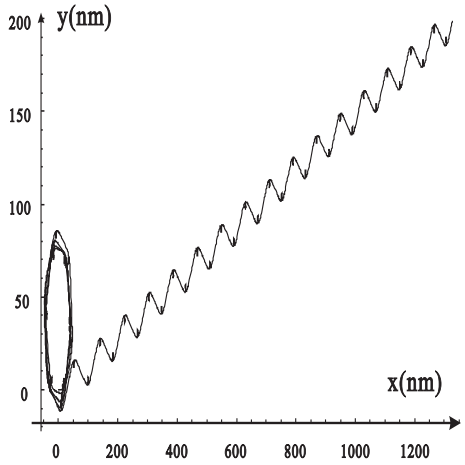

Fig. 7: DNA configuration with initial curvature $\kappa(0)$=0 nm^{-1}.

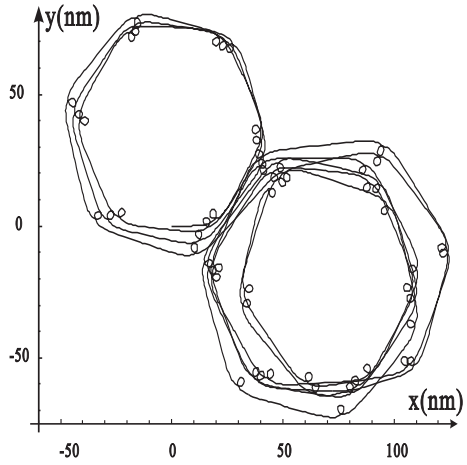

Fig. 10: DNA configuration with a=1 nm and b=1.5 nm.

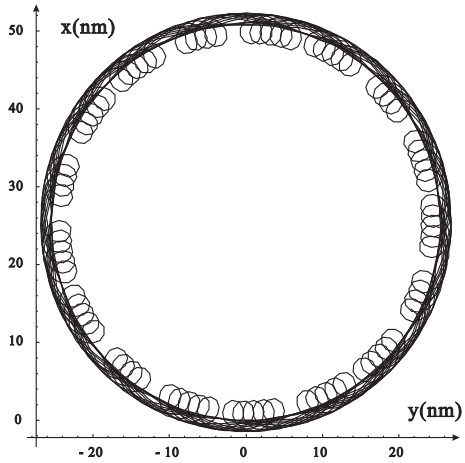

Fig. 8: DNA configuration with initial curvature $\kappa(0)$=0.005 nm^{-1}.

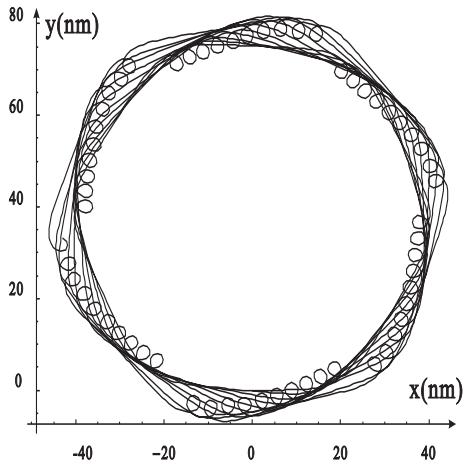

Fig. 11: DNA configuration with a=1 nm and b=3 nm.

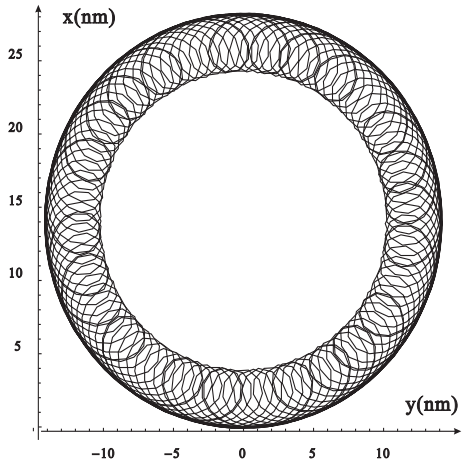

Fig. 9: DNA configuration with initial curvature $\kappa(0)$=0.05 nm^{-1}.

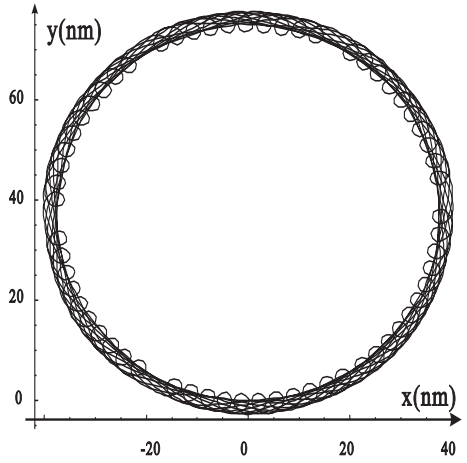

Fig. 12: DNA configuration with a=1 nm and b=9 nm.

3.3 Effects of salt solution concentration

A series of experiments have shown that, as a polyelectrolyte, geometrical configuration of DNA in a multivalent salt solution is directly influenced by the ionic concentration of the salt solution [30, 31]. At low salt, the DNA chain manifests itself in a sparse interwound configuration; while the high salt, the DNA condenses into a toroidal structure [32]. In this section, we will discuss the effect of ionic concentration on the equilibrium configuration of DNA segment.

The relationship between the interfacial tension σ can be characterized by the Gibbs adsorption equation, which reads [33]

$$d\sigma = -RT\Gamma_s d\ln c, \tag{11}$$

where c is the concentration, Γ denotes adsorbed amount, T and R are absolute temperature and the gas constant, respectively. Calculate the above equation, we can obtain [32]

$$\sigma = \sigma_0 - \Gamma_{max} RT \ln(1 + Kc), \tag{12}$$

where σ_0 is the interfacial tension of pure solvent, Γ_max and K denote the maximum concentration when the solution arrives at saturation state and the absorption constant. In this calculating, $\Gamma_s = \Gamma_{max} Kc/(1 + Kc)$ is recalled.

The influence of ionic concentration on the elastic modulus of polymer filament is not ignored, as shown in the experiment [34], C. G. Baumann measured the elastic modulus in the salt solution with different ionic strength, and find that the ionic concentration is lowed, the elastic modulus decreases.

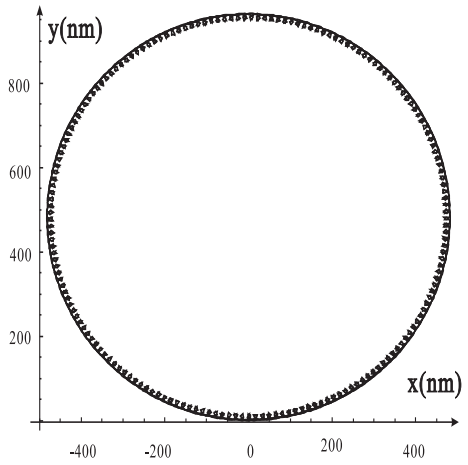

Fig. 13: DNA configuration with ionic strength 1.86 mM.

Taking $\Gamma_{max} = 5.35 \times 10^{-6}\ mol/m^2$, $K = 100$, $T = 22°C$ and $\kappa(0) = \kappa_0 = 0.01\ nm^{-1}$, we consider the reconfiguration of DNA segments in the Nacl salt solution with ionic strength $1.86\ nM$ and $186\ nM$, which are shown in Fig. 13 and 14. The configuration is greatly different with each other and it is easy to find the great influence of ionic strength on the reconfiguration, which shows a fairly well agreement with experimental data [31].

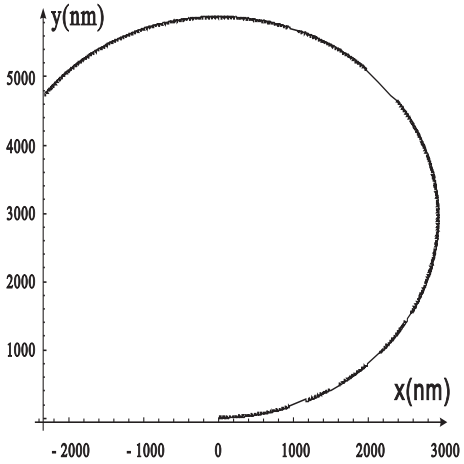

Fig. 14: DNA configuration with ionic strength 186 mM.

3.4 DNA loop

As is known to all, the protein–DNA interaction is attracting increasing interest [35]. And a protein binding to DNA often results in formation of a DNA loop [28, 36, 35]. A segment of DNA protein molecule or when the DNA gets wound around a large multiprotein aggregate, such as the nucleosome [37]. In order to analyze DNA loops under different solution environment, we can establish a simplified model, which two end points of DNA segment are fixed, to observe DNA reconfiguration under different interfacial environment. There are a number of approaches available for solving this type of boundary value problem [38]. The solution steps used, based on the shooting method, are using in the following.

we take the total arc length is $5\pi\ nm$, the initial curvature 0.001 nm^{-1}, $a = b$=1 nm, the coordinates of both end points of DNA elastic rod are (0,0) and (0,1) which are also the operator sites of protein clamp. when $\sigma = 2.6 \times 10^{-2}\ nN/nm$ and E=0.16 nN/nm^2, we can calculate that only $F_1(0)$=0.0058 nN, $F_3(0)$= -0.0966 nN, $\kappa(0)$=0.4929 nm^{-1} does the configuration form a DNA loop with the protein which is shown in Fig. 13. Through calculating, we can get $F_1(0)$=0, $F_3(0)$=-0.0294 nN, $\kappa(0)$=0.4518 nm^{-1} when the interfacial energy factor reduces to $1 \times 10^{-3}\ nN/nm$ and the bending stiffness increases to $16nm^{-1}$, which simulates the solution environment altering. Fig. 14 compared the two curvatures of the two cases, which shows the effect of solution on

the DNA loops configuration. It is easy to find that the DNA loop exerts diverse forces upon the protein clamp at the each end under different solution environment.

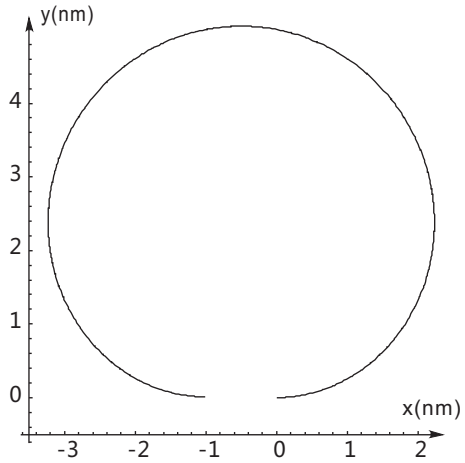

Fig. 15: DNA loop configuration with $\sigma = 2.6 \times 10^{-2}$ and $E = 0.16nm^{-1}$.

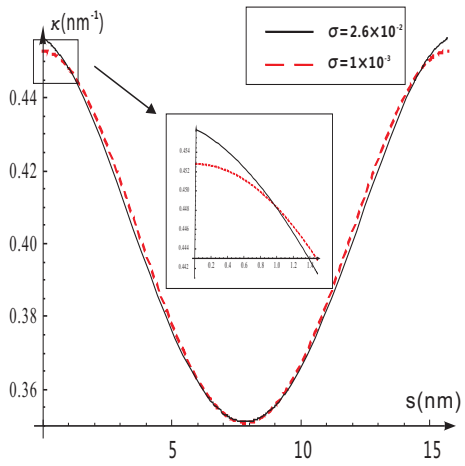

Fig. 16: Comparing DNA loop configuration with $\sigma = 2.6 \times 10^{-2}$ $E = 0.16nm^{-1}$ and $\sigma = 1 \times 10^{-3}$ $E = 1.6nm^{-1}$.

4 Conclusion

A model of DNA elastic rod, which characterizes DNA reconfiguration in solution, is established to determine the equilibrium configuration under the action of interfacial interactions. Some conclusions are summarized as follows:

1. The traction on the central axis curve of DNA elastic rod presented by Zaixing Huang [11] are incorrect, and new numerical results, which for the values given by Zaixing Huang do not give rise to the physical behavior observed for DNA by the author.

2. Toroidal DNA was observed by new parameters. And the effects of solution environment, initial curvature, anisotropic modulus of DNA bending and ionic strength on DNA reconfiguration are studied. DNA segment will undergo a series of alteration with the change of the solution environment, initial restriction, the shape of DNA rod cross-section and salt solution concentration.

3. DNA segments undergo condensed configurations under the traction induced by interfacial energy and elastic strain.

4. DNA loop exerts different forces upon the protein clamp at the each end under different solution environment.

Finally, it should be noted that, this is only a coarse-grained model characterizing interaction potentials between DNA segments and solution, and the deformations of elastic under applied end forces[15] should be considered into future models.

Acknowledgements: My conscience will not serve me well if I failed to extend my sincerest thanks and appreciations to the institutions and people who have worked collaboratively to see that the aims and objectives to complete this research is attained. The authors are grateful to the reviewer for comments and suggestions. Project 11372210 supported by the National Nature Science Foundation of China, and Project 20120032110010 supported by the Specialized Research Fund for the Doctoral Program of Higher Education of China.

References:

[1] J. Nishimura, Y. Murakami, K. Taroh, Paroxysmal nocturnal hemoglobinuria: an acquired genetic disease, *American journal of hematology*, 62(3), 1999, pp. 175–182.

[2] Y. Yoichi, S. Kenji, Prediction of genomic methylation status on CpG islands using DNA sequence features, *WSEAS Transactions on Biology and Biomedicine*, 5(7), 2008, pp. 153–162.

[3] I. Pesek, J. Žerovnik, New spectral numerical characterization of DNA sequences, *WSEAS Transactions on Biology and Biomedicine*, 5(10), 2008, pp. 261–270.

[4] J. F. Marko, E. D. Siggia, Statistical mechanics of supercoiled DNA, *Physical Review E*, 52(3), 1995, pp. 2912.

[5] J. E. Hearst, N. G. Hunt, Statistical mechanical theory for the plectonemic DNA supercoil, *The Journal of chemical physics*, 95, 1991, pp. 9322.

[6] B. Fain, J. Rudnick, S. Östlund, Conformations of linear DNA, *Physical Review E*, 55(6), 1997, pp. 7364.

[7] X. Zhou, J. Liu, Stability analysis of kinked DNA with generalized rod model, *Physica E: Low-dimensional Systems and Nanostructures*, 62(3), 2013, pp. 152–156.

[8] S. B. Smith, Y. Cui, C. Bustamante, Overstretching B-DNA: the elastic response of individual double-stranded and single-stranded DNA molecules, *Science*, 271(5250), 1996, pp. 795–799.

[9] C. Bustamante, Direct observation and manipulation of single DNA molecules using fluorescence microscopy, *Annual review of biophysics and biophysical chemistry*, 20(1), 1991, pp. 415–446.

[10] S. B. Smith, L. Finzi, C. Bustamante, Direct mechanical measurements of the elasticity of single DNA molecules by using magnetic beads, *Science*, 258(5085), 1992, pp. 1122–1126.

[11] Z. Huang, Modulating DNA configuration by interfacial traction: an elastic rod model to characterize DNA folding and unfolding, *Journal of biological physics*, 37(1), 2011, pp. 79–90.

[12] Y. Shi, J. E. Hearst, The Kirchhoff elastic rod, the nonlinear Schrödinger equation and DNA supercoiling, *The Journal of chemical physics*, 101(6), 1994, pp. 5186–5199.

[13] W. Wang, Q. Zhang, Q. Xie, Analytical reduction of the non-circular Kirchhoff elastic rod model with the periodically varying bending rigidities, *Physica Scripta*, 87(4), 2013, pp. 045402.

[14] Y. Liu, Y. Xue, Some Aspects of Research on Mechanics of Thin Elastic Rod, *Journal of Physics: Conference Series*, 448(1), 2013, pp. 012001.

[15] A. G. Cherstvy, Torque-induced deformations of charged elastic DNA rods: thin helices, loops, and precursors of DNA supercoiling, *Journal of biological physics*, 37(2), 2011, pp. 227–238.

[16] W. K. Olson, N. L. Marky, R. L. Jernigan, Influence of fluctuations on DNA curvature: a comparison of flexible and static wedge models of intrinsically bent DNA, *Journal of molecular biology*, 232(2), 1993, pp. 530–554.

[17] W. K. Olson, A. A. Gorin, X. J. Lu, DNA sequence-dependent deformability deduced from protein–DNA crystal complexes, *Proceedings of the National Academy of Sciences*, 95(19), 1998, pp. 11163–11168.

[18] T. M. Jovin, D. M. Soumpasis, The Transition Between B-DNA and Z-DNA, *Annual Review of Physical Chemistry*, 38(1), 1987, pp. 521–558.

[19] J. C. G. Montoro, J. L. F. Abascal, The free energy difference between simple models of B-and Z-DNA: Computer simulation and theoretical predictions, *The Journal of chemical physics*, 106(19), 1997, pp. 8239–8253.

[20] Y. Liu, Nonlinerar Mechanics of Thin Elastic Rod: Theoretical Basis of Mechanical Model of DNA (in Chinese), *Tsinghua Press*, Beijing, 2006.

[21] V. A. Marichev, Current state and problems in the surface tension of solids, *Colloids and Surfaces A: Physicochemical and Engineering Aspects*, 345(1), 2009, pp. 1–12.

[22] E. S. De, G. Maciel, First order unstructured algorithms applied to the solution of the euler equations in three-dimensions, *WSEAS Transactions on Mathematics*, 11(3), 2012, pp. 183–203.

[23] V. A. Bloomfield, DNA condensation, *Current opinion in structural biology*, 6(3), 1996, pp. 334–341.

[24] V. A. Bloomfield, DNA condensation by multivalent cations, *Biopolymers*, 44(3), 1997, pp. 269–282.

[25] C. Bustamante, Direct observation and manipulation of single DNA molecules using fluorescence microscopy, *Annual review of biophysics and biophysical chemistry*, 20(1), 1991, pp. 415–446.

[26] A. M. Carnerup, M. L. Ainalem, V. Alfredsson, T. Nylander, Condensation of DNA using poly (amido amine) dendrimers: effect of salt concentration on aggregate morphology, *Soft Matter*, 7(2), 2011, pp. 760–768.

[27] A. R. Leach, Molecular modelling: principles and applications, *Prentice hall*, London, 2001.

[28] A. Balaeff, L. Mahadevan, K. Schulten, Modeling DNA loops using the theory of elasticity, *Physical Review E*, 73(3), 2006, pp. 031919.

[29] A. T. R. Strick, J. F. Allemand, D. Bensimon, Stress-induced structural transitions in DNA and proteins, *Annual review of biophysics and biomolecular structure*, 29(1), 2000, pp. 523–543.

[30] T. Schlick, B Li, W. K. Olson, The influence of salt on the structure and energetics of supercoiled DNA, *Biophysical journal*, 67(6), 1994, pp. 2146–2166.

[31] C. C. Conwell, I. D. Vilfan, N. V. Hud, Controlling the size of nanoscale toroidal DNA condensates with static curvature and ionic strength, *Proceedings of the National Academy of Sciences*, 100(16), 2003, pp. 9296–9301.

[32] Y. Xiao, Z. X. Huang, S. N. Wang, An elastic rod model to evaluate effects of ionic concentration on equilibrium configuration of DNA in salt solution, *Journal of Biological Physics*, 40, 2014, pp. 179–192.

[33] F. T. Zhang, Fundamentals of molecular interface chemistry (in Chinese), *Shanghai Scientific and Technology Literature Publishing House*, Shanghai, 2006.

[34] C. G. Baumann, S. B. Smith, V. A. Bloomfield, C. Bustamante, Ionic effects on the elasticity of single DNA molecules, *Proceedings of the National Academy of Sciences*, 94(12), 1997, pp. 6185–6190.

[35] S. Yu, S. Wang, R. G. Larson, Proteins searching for their target on DNA by one-dimensional diffusion: overcoming the speed-stability paradox, *Journal of biological physics*, 39(3), 2013, pp. 565–586.

[36] J. M. G. Vilar, L. Saiz, DNA looping in gene regulation: from the assembly of macromolecular complexes to the control of transcriptional noise, *Current opinion in genetics & development*, 15(2), 2005, pp. 136–144.

[37] K. Luger, Structure and dynamic behavior of nucleosomes, *Current opinion in genetics & development*, 13(2), 2003, pp. 127–135.

[38] O. Martin, Boundary Problems for Stationary Neutron Transport Equations Solved by Homotopy Perturbation Method, *WSEAS Transactions on Mathematics*, 12(5), 2013, pp. 521–530.